Eye and Brain

Dovepress
open access to scientific and medical research

Open Access Full Text Article

ORIGINAL RESEARCH

VGLUT2 mRNA and protein expression in the visual thalamus and midbrain of prosimian galagos (*Otolemur garnetti*)

This article was published in the following Dove Press journal:
Eye and Brain
18 March 2011
Number of times this article has been viewed

Pooja Balaram[1]
Toru Takahata[1]
Jon H Kaas[1,2]

[1]Department of Psychology, [2]Department of Cell and Molecular Biology, Vanderbilt University, Nashville, TN, USA

Abstract: Vesicular glutamate transporters (VGLUTs) control the storage and presynaptic release of glutamate in the central nervous system, and are involved in the majority of glutamatergic transmission in the brain. Two VGLUT isoforms, VGLUT1 and VGLUT2, are known to characterize complementary distributions of glutamatergic neurons in the rodent brain, which suggests that they are each responsible for unique circuits of excitatory transmission. In rodents, VGLUT2 is primarily utilized in thalamocortical circuits, and is strongly expressed in the primary sensory nuclei, including all areas of the visual thalamus. The distribution of VGLUT2 in the visual thalamus and midbrain has yet to be characterized in primate species. Thus, the present study describes the expression of *VGLUT2* mRNA and protein across the visual thalamus and superior colliculus of prosimian galagos to provide a better understanding of glutamatergic transmission in the primate brain. VGLUT2 is strongly expressed in all six layers of the dorsal lateral geniculate nucleus, and much less so in the intralaminar zones, which correspond to retinal and superior collicular inputs, respectively. The parvocellular and magnocellular layers expressed *VGLUT2* mRNA more densely than the koniocellular layers. A patchy distribution of VGLUT2 positive terminals in the pulvinar complex possibly reflects inputs from the superior colliculus. The upper superficial granular layers of the superior colliculus, with inputs from the retina, most densely expressed VGLUT2 protein, while the lower superficial granular layers, with projections to the pulvinar, most densely expressed *VGLUT2* mRNA. The results are consistent with the conclusion that retinal and superior colliculus projections to the thalamus depend highly on the VGLUT2 transporter, as do cortical projections from the magnocellular and parvocellular layers of the lateral geniculate nucleus and neurons of the pulvinar complex.

Keywords: lateral geniculate nucleus, superior colliculus, pulvinar, primate, glutamate

Introduction

The primary mode of excitatory neurotransmission in the central nervous system is performed through the release of glutamate from presynaptic vesicles and its postsynaptic uptake through ionotropic or metabotropic glutamate receptors. The presynaptic release of glutamate is controlled by a family of vesicular glutamate transporters (VGLUTs) that modulate the packaging and transport of glutamate into synaptic vesicles.[1] Three isoforms, VGLUT1, VGLUT2, and VGLUT3, have been previously identified, each classifying a unique subset of glutamatergic projections. VGLUT1 is primarily utilized by projections from the cerebral cortex, cerebellum and hippocampus, while VGLUT2 is primarily employed by projections from the midbrain, thalamus, brainstem and spinal cord. VGLUT3 differs from VGLUT1 and VGLUT2 in that it does not appear in glutamatergic neurons, it is mainly found in a subpopulation of

Correspondence: Pooja Balaram
Vanderbilt University, 301 Wilson Hall, 111 21st Avenue South, Nashville, TN 37203, USA
Tel +1 508 314 3030
Fax +1 615 343 8449
Email pooja.balaram@vanderbilt.edu

cholinergic neurons of the caudate-putamen and serotonergic neurons of the raphe nuclei.[2] The unique distributions of each VGLUT isoform may indicate specialized modes of glutamatergic transport and transmission that are modulated by these transporters.

In previous studies in rodents, *VGLUT2* mRNA is expressed in the thalamus, brainstem, and deep cerebellar nuclei, and VGLUT2 protein is primarily confined to the expected subthalamic and thalamocortical projections.[2] In the visual subcortical nuclei, *VGLUT2* mRNA is strongly expressed in the dorsal lateral geniculate nucleus (dLGN), the superior colliculus (SC), and the lateral posterior nucleus (LP) or visual pulvinar.[3] VGLUT2 protein is also strongly expressed in those three nuclei.[4] VGLUT2 has also been associated with a higher probability of synaptic release and functionally distinct synaptic release sites in the brains of adult rodents when compared to the other two VGLUT isoforms.[2,5] The discrete distribution of *VGLUT2* mRNA and protein in the central nervous system of rodents suggests this isoform plays a unique role in glutamate release and excitatory neurotransmission.

Little work has been done on the distribution of VGLUT2 in primate species. The few studies that discuss VGLUT distributions in primates focus on their immunoreactivity in cortex and do not discuss their expression in thalamic nuclei.[6–9] Moreover, only one study to date considers the gene expression of VGLUTs in primate sensory pathways.[10] In order to expand on the knowledge of VGLUT2 distributions in primate species, we investigated the expression of *VGLUT2* mRNA and protein across the major visual subcortical areas in prosimian galagos (*Otolemur garnetti*). Galagos are highly visual nocturnal primates with a visual thalamus[6] and a distribution of cortical areas that are organized much as they are in anthropoid primates.[7,11] Galagos also represent the prosimian branch of the primate radiation, the branch that appears to be the most evolutionarily conserved and most similar to the early ancestors of all primates.[12] Previous work on the neocortex of galagos shows that VGLUT2 protein is abundant in layer 4 of striate cortex and, to a lesser extent, in higher order visual areas, suggesting that VGLUT2 is primarily located in thalamocortical projections.[7] This interpretation is consistent with rodent studies of VGLUT2 protein expression in cortical areas.[4,13] Our examination of *VGLUT2* mRNA and protein expression in thalamic visual regions similarly supports rodent findings; *VGLUT2* mRNA and protein are strongly expressed in visual relay nuclei in the thalamus, and are consistent with known afferent and efferent projections to cortical and thalamic areas. Moreover, differences in VGLUT2 gene expression and immunoreactivity occur across layers of the dorsal lateral geniculate nucleus and superior colliculus, and within parts of the pulvinar complex, providing additional insights into the functional organization of visual structures in primates.

Materials and methods

VGLUT2 mRNA and protein expression were studied in three adult prosimian galagos (*Otolemur Garnetti*). All experimental procedures were approved by the Vanderbilt Institutional Animal Care and Use Committee and followed the guidelines published by the National Institutes of Health.

Tissue preparation

Each animal was given a lethal dose of sodium pentobarbital (80 mg/kg) and transcardially perfused with 0.1 M phosphate-buffered saline (PBS), followed by 4% paraformaldehyde in sterile PBS. The brain was removed from the skull, postfixed for 2–4 hours in 4% paraformaldehyde in sterile PBS, and then cryoprotected in 30% sucrose in sterile PBS overnight. The subcortical region was separated from the two cortical hemispheres and cut into 40 μm coronal sections on a sliding microtome. The subcortical sections were then separated into six series for further study.

Histochemistry

One series of sections from each animal was processed for Nissl substance with thionin to determine the cellular architecture and laminar organization of subcortical structures. Another series was processed for cytochrome oxidase (CO) as an additional aid in identifying the subcortical structures.[14]

In situ hybridization

VGLUT2 mRNA distribution was examined in one series of brain sections from each animal using in situ hybridization (ISH). A digoxigenin (DIG)-labeled riboprobe for *VGLUT2* was prepared using galago liver cDNA libraries with reverse transcriptase-polymerase chain reaction (RT-PCR) and conventional TA cloning techniques, and labeled using a DIG-dUTP labeling kit (Roche Diagnostics, Indianapolis, IN). The forward and reverse primers used for *VGLUT2* were GCCATCGTGGACATGGTCAA and ATAACTCCAC CATAGTGGAC respectively, which targeted position 693-1888 of human *VGLUT2* (NM_020346). BLAST assessments of this region of galago *VGLUT2* (JF290396) to those of macaque *VGLUT2* (XM_002799604) and human *VGLUT2* revealed 99% homology for both comparisons.

Similar assessments of other members of the VGLUT family showed 72% homology between human *VGLUT1* (AB032436) and *VGLUT2*, and 75% homology between human *VGLUT3* (AJ459241) and *VGLUT2*, indicating that although VGLUT2 shows significant homology between species, the protein is genetically distinct from other VGLUT isoforms. Additionally, the *VGLUT2* probe used in this study exhibited distinct signals from those of *VGLUT1*, as previously shown.[10]

ISH was carried out as described previously.[15] Briefly, free-floating sections were soaked in 4% paraformaldehyde/0.1 M phosphate buffer (pH 7.4) overnight at 4°C and treated with 10 µg/mL proteinase K for 30 minutes at 37°C. After acetylation with 0.25% acetic anhydride in 0.9% triethanolamine and 0.12% hydrochloric acid, the sections were incubated in hybridization buffer (pH 7.5) containing 5× saline sodium citrate (SSC; 150 mM sodium chloride, 15 mM sodium citrate, pH 7.0), 50% formamide (FA), 2% blocking reagent (Roche Diagnostics), 0.1% *N*-lauroylsarcosine (NLS), 0.1% sodium dodecyl sulphate (SDS), 20 mM maleic acid buffer, and 1 µg/mL of the appropriate DIG-labeled riboprobe. Sections were hybridized with the probe overnight at 60°C and washed by successive immersion in 2× SSC, 50% FA, 0.1% NLS for 20 minutes at 60°C. Nonspecific mRNA was removed with 20 µg/mL RNase A in RNase A buffer (10 mM Tris-HCl, 10 mM ethylenediamine-N,N,N′,N′-tetraacetic acid (EDTA), 500 mM NaCl; pH 8.0) for 15 minutes at 37°C and sections were washed twice in 2× SSC, 50% FA, 0.1% NLS, followed by two more washes in 0.2× SSC, 50% FA, 0.1% NLS, for 20 minutes each. Hybridized mRNA signals were visualized by alkaline phosphatase (AP) immunohistochemical staining using a DIG detection kit (Roche Diagnostics). Sections were mounted onto gelatin-subbed glass slides and dehydrated through a graded ethanol series (70% for 5 minutes, 95% for 10 minutes, 100% for 10 minutes), cleared in xylene (5 minutes), and then coverslipped with Permount.

Immunohistochemistry

One series of brain sections from each animal was processed for immunohistochemical localization of VGLUT2 protein. Sections were rinsed in 0.1 M PBS and quenched in 0.3% hydrogen peroxide, rinsed again in 0.1 M PBS, and incubated for 2 hours at room temperature in blocking solution (5% normal horse serum, 0.5% Triton X-100 in 0.1 M PBS). Sections were then incubated overnight in a primary antibody solution of 1:5000 goat anti-mouse VGlUT2 (Millipore, Billerica, MA) in blocking solution, rinsed in PBS, and incubated for 2 hours at room temperature in 1:200 peroxidase anti-goat IgG in blocking solution. Sections were rinsed in PBS and then incubated for 1 hour at room temperature in ABC reaction (ABC kits; Vector, Burlingame, CA). Immunoreactivity was then visualized by developing sections in diaminidobenzidine (DAB) solution (0.2 mg/mL DAB, 0.1% hydrogen peroxide, 1% nickel ammonium sulfate). Sections were rinsed in water to stop the DAB reaction, mounted on gelatin-subbed glass slides, dehydrated though a graded ethanol series (70% for 3 minutes, 95% for 6 minutes, 100% for 6 minutes) followed by xylene (5 minutes), and coverslipped with Permount.

Light microscopy

Digital photomicrographs of relevant thalamic and midbrain structures were captured using a Nikon DXM2200 camera (Nikon, Melville, NY) mounted on a Nikon E800 microscope. The images were adjusted for brightness and contrast using Adobe Photoshop (Adobe Systems, San Jose, CA), but were not otherwise altered.

Results

The present study characterizes the distribution of VGLUT2 mRNA and protein within the visual thalamus and superior colliculus of prosimian galagos. Overall, VGLUT2 mRNA and protein are strongly expressed in the lateral geniculate nucleus, superior colliculus and pulvinar complex, but further analysis reveals a unique expression pattern for each layer or subdivision of the three regions. Additionally, sense and antisense labeling confirmed probe specificity to *VGLUT2* mRNA (Figure 1). The detailed expression patterns of each subcortical area are discussed below.

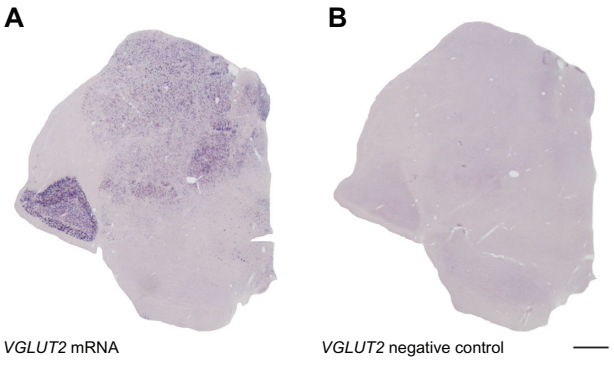

Figure 1 Coronal brain sections through the caudal thalamus of a galago. Sense and anti-sense probes for *VGLUT2* confirm staining specificity for *VGLUT2* mRNA and lack of secondary reactivity due to staining techniques. **A**) Anti-sense *VGLUT2* probe stains *VGLUT2* mRNA in the thalamus. **B**) Sense *VGLUT2* probe does not stain *VGLUT2* mRNA and does not show any secondary signal in the thalamus. Scale bar is 1 mm. The thalamic midline is to the right.

Lateral geniculate nucleus

The dorsal lateral geniculate nucleus (LGN) of galagos is characterized by six layers, each of which receives monocular input from the contralateral or ipsilateral eye and projects to layer IV of the primary visual cortex.[16] As described previously,[17] the layers of the LGN are organized from ventral to dorsal as follows: external magnocellular (ME), internal magnocellular (MI), internal parvocellular (PI), internal koniocellular (KI), external koniocellular (KE), and external parvocellular (PE). Low magnification images of coronal sections through the LGN show its laminar organization (Figures 2 and 3). In rostral sections, LGN layers are wide medially where central vision is represented and narrow laterally where peripheral vision is represented (Figure 2). In caudal sections of the LGN, layers remain the same size from the medial edge to the lateral edge and are easily distinguishable from each other (Figure 3). A sublayer or leaflet of MI, which lies ventral to ME, is visible in caudal sections of the LGN, especially in the VGLUT2 preparations (Figures 3A–3D). This sublayer of MI appears medially where MI proper thins to a narrow band.

CO distribution in the galago LGN has been characterized previously.[18,19] Our results also defined a series of darkly stained layers separated by lightly stained interlaminar zones (Figures 2A and 3A). The CO-rich M and P layers were easily distinguishable from their CO-poor surroundings and appeared as four distinct bands in all sections. The K layers, however, were much lighter in CO sections and were barely distinguishable from their surrounding interlaminar zones. In Nissl preparations, the LGN layers were densely packed with darkly stained cell bodies, while the interlaminar zones were lighter in color and diffusely populated with smaller, lightly stained cell bodies (Figures 2B and 3B).

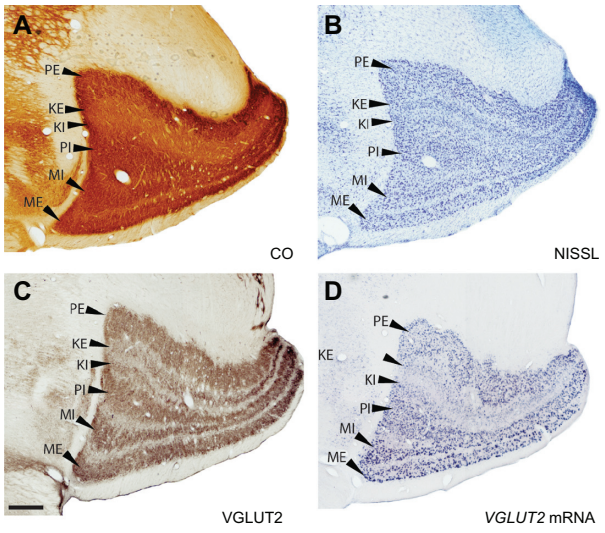

Figure 2 Serial sections through part of the rostral lateral geniculate nucleus (LGN) stained for (**A**) cytochrome oxidase (CO), (**B**) Nissl, (**C**) VGLUT2 protein and (**D**) *VGLUT2* mRNA. Scale bar is 0.5 mm. Coronal sections, lateral is right.

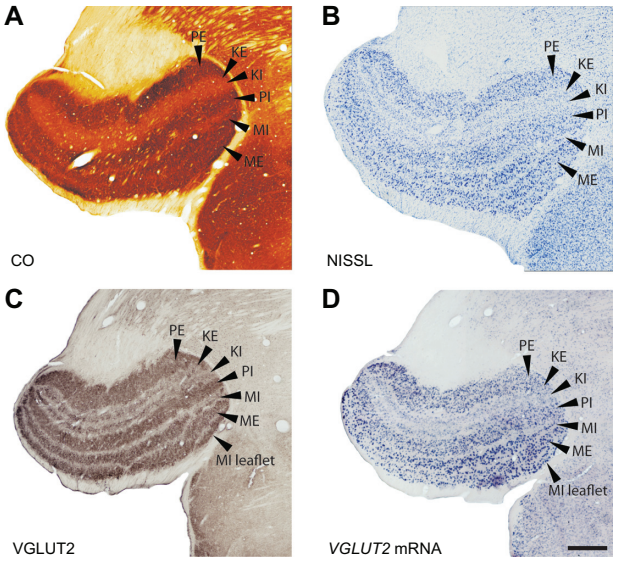

Figure 3 Serial sections through the caudal lateral geniculate nucleus (LGN) stained for (**A**) cytochrome oxidase (CO), (**B**) Nissl, (C) VGLUT2 protein and (D) *VGLUT2* mRNA. Scale bar is 0.5 mm. Coronal sections, lateral is left.

The cell bodies in the parvocellular and magnocellular layers of the LGN stained for *VGLUT2* mRNA (Figures 2D and 3D) suggesting that VGLUT2 is the primary glutamate transporter utilized by LGN projections to layer IV of V1. The magnocellular layers were characterized by large cells that stained densely for *VGLUT2* mRNA and tended to group together in short strings (Figure 4E). This clustered organization appeared to be unique to the magnocellular layers of the LGN (Figure 4). In the parvocellular layers, cells stained for *VGLUT2* mRNA were smaller and evenly distributed, but showed an intensity of staining nearly equal to those of cells in the magnocellular layers (Figures 4A and 4C). In the K layers, cells stained for *VGLUT2* mRNA were widespread and evenly distributed, but individual cells were weakly stained in comparison to individual cells from the M and P layers (Figure 4B). Some of the small cells of the sparsely populated interlaminar zones of the LGN stained weakly for *VGLUT2* mRNA (Figures 4A–4E). Neurons in both the K layers and the interlaminar zones project to layers I, II, and III of V1,[16] so their sparse *VGLUT2* mRNA distribution is consistent with the weak VGLUT2-ir previously described in those neocortex layers.[7]

The differences in cell sizes between M, P, and K layers were clearly visible in sections stained for *VGLUT2* mRNA (Figure 5A). M cells were the largest in area and diameter, and their cytoplasm stained darkly for *VGLUT2*

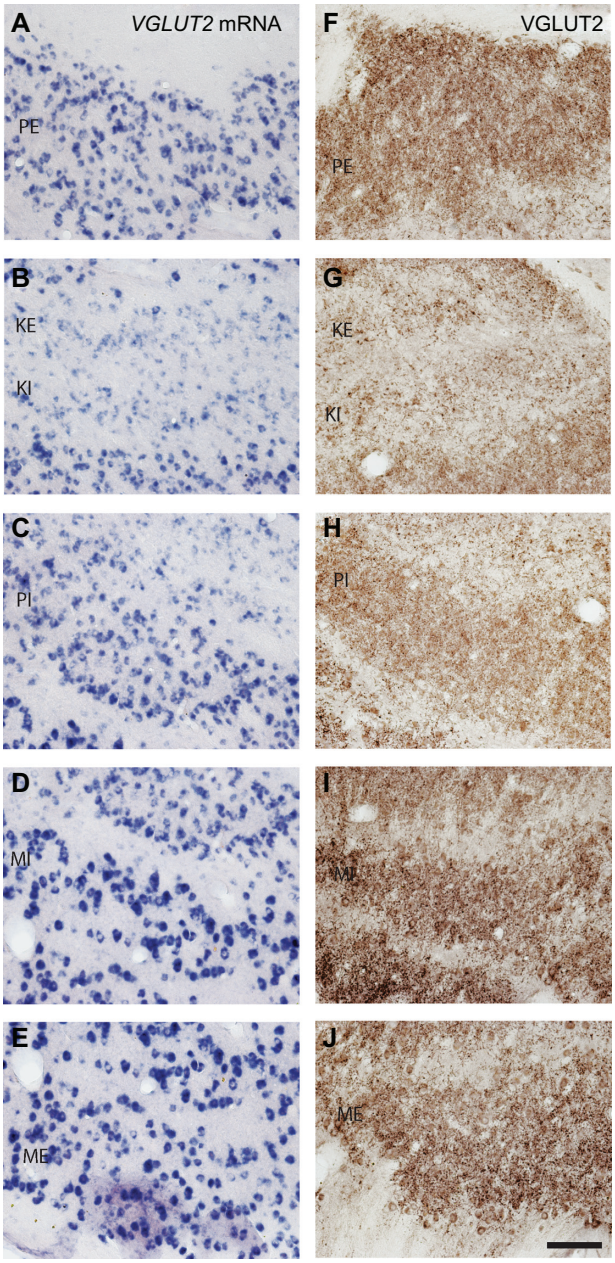

Figure 4 *VGLUT2* mRNA (**A–E**) and protein (**F–J**) expression in each layer of the LGN. Scale bar is 100 μm.

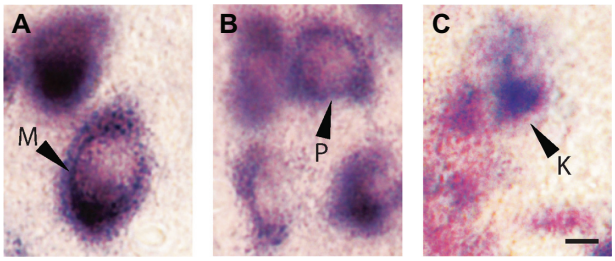

Figure 5 LGN cell types can be differentiated according to pattern of staining for *VGLUT2* mRNA. **A**) M cells are large and exhibit strong nuclear staining for *VGLUT2* mRNA. **B**) P cells are slightly smaller but also show intense staining for *VGLUT2*. **C**) K cells are the smallest of all three and show weak, diffuse staining for *VGLUT2*. Scale bar is 50 μm.

mRNA (Figure 5A). P cells were medium in size and stained less intensely (Figure 5B), while K cells were the smallest in size and stained weakly for *VGLUT2* mRNA (Figure 5C). This is consistent with the differences in sizes of M, P, and K cells in the LGN of galagos[20] and other primates described previously.[21]

When stained for VGLUT2 protein, all layers of the LGN were easily distinguishable by their strong VGLUT2 immunoreactivity (Figures 2C and 3C). The M layers of the LGN were characterized by large cell bodies surrounded by dense puncta of VGLUT2-stained terminals (Figures 4I, 4J and 6C), and had the largest proportion of VGLUT2-stained terminals compared to the other layers (Figures 4F–4J). The P layers of the LGN were less densely stained for VGLUT2 protein, but still showed intense staining of glutamatergic terminals and diffuse staining of cell bodies across both layers (Figures 4F and 4H). The K layers of the LGN were less densely stained for VGLUT2 protein (Figures 2C and 3C). At a higher magnification, it was apparent that staining is confined to sparse terminals within the layers and does not appear to be in cell bodies (Figure 4I). In contrast to the layers of the LGN, the interlaminar zones showed sparse immunoreactivity for VGLUT2 protein (Figure 6A). However, when viewed at higher magnification, VGLUT2 terminals were visible throughout the interlaminar zones (Figure 6C).

Pulvinar

The pulvinar complex in galagos is traditionally divided into three regions, the medial pulvinar (PM), lateral pulvinar (PL), and the inferior pulvinar (PI).[22–25] The architecture of these three regions in CO- and Nissl-stained sections has been described previously by Wong et al.[6] Our results were consistent with those findings (Figures 7A and 7B) and we could not further subdivide the pulvinar with these two preparations.

When stained for *VGLUT2* mRNA, PM and PL both showed a uniform distribution of stained cells, and were barely distinguishable from each other by staining intensity (Figure 7C). Higher magnification images show that PL cells stained slightly darker than PM cells (Figure 8A), but quantitative measures would be needed to justify this conclusion. Although the staining density of *VGLUT2* mRNA-positive cells was greater in PL compared to PM, this could be due to the higher cell density characteristic of this region (Figures 7A, 7C, 8A and 8B). PI is separated from PM and PL by the brachium of the SC, which was relatively free of cells positive for *VGLUT2* mRNA. PI could also be distinguished from surrounding thalamic nuclei by

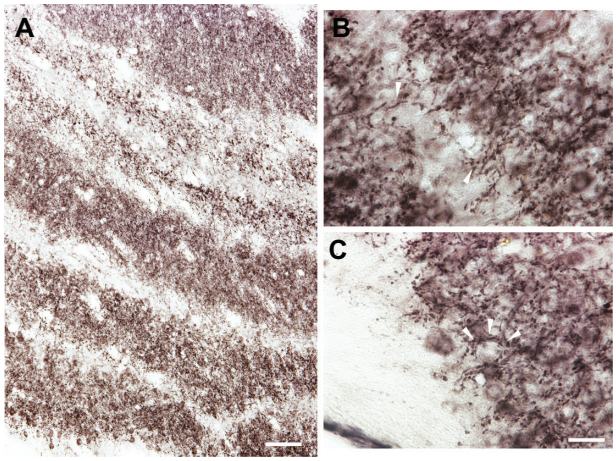

Figure 6 Laminar pattern of VGLUT2 immunoreactivity across the LGN. **A**) VGLUT2 is strongly expressed in each layer of the LGN but less so in the interlaminar zones. However, high magnification (**B**) shows VGLUT2-positive terminals throughout the interlaminar zones. **C**) VGLUT2-positive terminals encircle labeled and unlabeled cells in the M layers of the LGN, but not in the P or K layers. Scale bar is (**A**) 250 μm and (**B–C**) 100 μm.

its distribution of strongly stained *VGLUT2* mRNA-positive cells. Further divisions of PI were unclear in this preparation, but varying densities of stained cells (Figure 8C) suggest that PI is not homogeneous in its organization.

All three divisions of the pulvinar complex exhibited strong immunoreactivity when stained for VGLUT2 protein (Figure 7D). PM, PL, and PI all showed even distributions of punctate VGLUT2-ir and darker background staining in comparison to surrounding fiber tracts and neighboring nuclei (with the exception of the LGN). VGLUT2-ir in each region was primarily confined to cell bodies and axons instead of terminals (Figure 9), suggesting that VGLUT2-ir in the pulvinar is more representative of VGLUT2 protein within projection

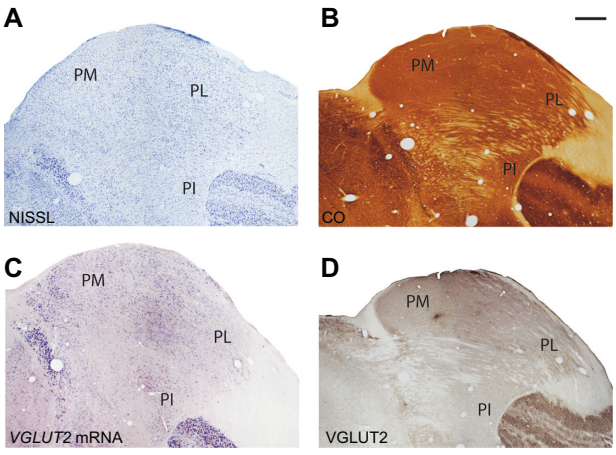

Figure 7 Serial sections through the pulvinar complex stained for (**A**) Nissl, (**B**) CO, (**C**) *VGLUT2* mRNA and (**D**) VGLUT2 protein. Scale bar is 1 mm. Coronal sections; medial is left. PM, PL, PI: medial, lateral, and inferior divisions of the pulvinar complex.

neurons and their axons in the pulvinar rather than efferent projections from other cortical or thalamic regions. However, in parts of the pulvinar, dense patches of VGLUT2-ir were observed (Figure 10). At higher magnification, these patches were identified as clusters of VGLUT2 positive terminals (Figure 11). These patches were most obvious in medial PL. However, similar patches appeared occasionally along the lateral edge of PL or in PI, but this was not consistent across all sections. Other than this patchy distribution, no further architectonic subdivisions of the pulvinar complex were identified from either of the VGLUT2 preparations.

Superior colliculus

The superior colliculus in the galago has been previously subdivided into seven distinct layers in CO and Nissl preparations[26,27] and our results are largely consistent with these previous findings (Figure 12). However, in CO-stained sections, the stratum griseum intermediale (SGI) could be further subdivided according to staining intensity into three sublayers. The dorsal and ventral outer sublayers were darkly stained while the middle sublayer was weakly stained for CO (Figure 12A). These sublayers were, however, indistinguishable in Nissl preparations (Figure 12B).

The stratum griseum superficiale (SGS) could be clearly divided into upper and lower sublayers according to the staining intensity of cells for *VGLUT2* mRNA (Figure 12C). The upper sublayer (uSGS) was characterized by weakly stained *VGLUT2* mRNA-positive cells while the lower sublayer (lSGS) was characterized by strongly stained *VGLUT2* mRNA-positive cells. These deeper, strongly stained cells likely project to the pulvinar.[28] The stratum opticum (SO) exhibited weak staining for *VGLUT2* mRNA and a more diffuse distribution of *VGLUT2* mRNA-positive cells. Each sublayer of the SGI showed a different staining distribution for *VGLUT2* mRNA-positive cells; the dorsal and ventral sublayers had slightly denser distributions of small, weakly-stained *VGLUT2* mRNA-positive cells while the middle sublayer had a sparse distribution of very large, strongly-stained *VGLUT2* mRNA-positive cells. This suggests that multiple subsets of cells in the SGI utilize VGLUT2, but additional markers would be required to fully differentiate their projections. Ventral to the SGI rests the stratum album intermediale (SAI) and the stratum griseum profundum (SGP), which were indistinguishable from each other in sections stained for *VGLUT2* mRNA. Both layers showed a diffuse distribution of small, weakly-stained cells. The stratum album profundum (SAP) below the SGP was free of cells stained for *VGLUT2* mRNA, which is consistent with its role as a

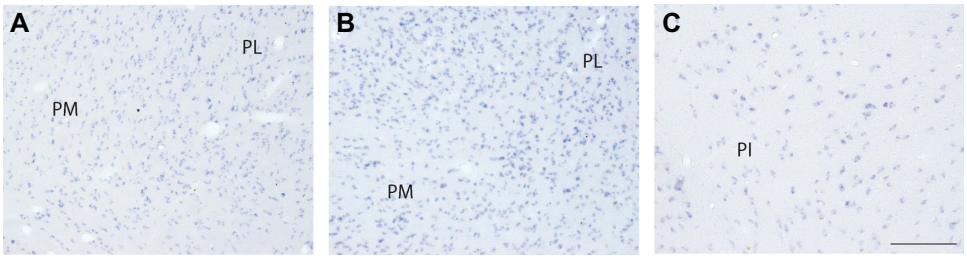

Figure 8 High magnification images of *VGLUT2* mRNA expression in each division of the pulvinar complex. **A**) PM and PL both show intense staining for *VGLUT2* mRNA but (**B**) PL shows a denser distribution of VGLUT2-positive cells than PM. **C**) PI stains variably in density and intensity for *VGLUT2* mRNA, indicated multiple populations of glutamatergic cells in this region. Scale bar is 250 μm.

white matter tract in the SC. The deepest layer of the SC, the periaqueductal gray (PAG), stained strongly for *VGLUT2* mRNA and could be separated into two zones according to staining density. The outer zone of the PAG (oPAG) showed a dense distribution of *VGLUT2* mRNA-positive cells while the thin inner zone (iPAG) was relatively free of cells positive for *VGLUT2* mRNA.

When stained for VGLUT2 protein, the layers of the SC could be similarly subdivided based on staining intensity (Figure 12D). The SZ was characterized by a thin, darkly stained band of VGLUT2-ir across the dorsal SC, which is consistent with its likely role as a recipient layer of retinotectal projections.[29,30] The SGS also stained strongly for VGLUT2 and could be clearly separated into two sublayers; uSGS appeared as a dark band across the dorsal SC while lSGS below it appeared as a slightly lighter band. In some sections, a darker layer of VGLUT2-ir appeared between the uSGS and lSGS but this was not consistent across the SC. In galagos, retinal projections from the contralateral eye terminate in the superficial half of the uSGS, while retinal projections from the ipsilateral eye terminate less densely and in the deeper half of the uSGS.[27] The SO showed diffuse projections that weakly stain for VGLUT2 protein. Ventral to the SO, the three layers of the SGI could be separated by their immunoreactivity; the outer sublayers appeared as darker bands of VGLUT2-ir while the middle sublayer appeared as a lighter band of VGLUT2-ir. Finally, the PAG showed strong, uniform VGLUT2-ir, but could not be subdivided into two zones in this preparation.

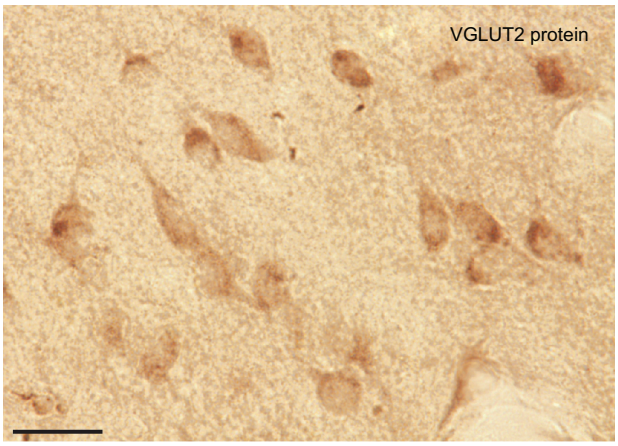

Figure 9 VGLUT2 protein expression in the pulvinar is largely confined to cell bodies and processes instead of terminals. Scale bar is 25 μm.

Discussion

The present study aimed to characterize the distribution of VGLUT2 mRNA and protein in the visual thalamus and

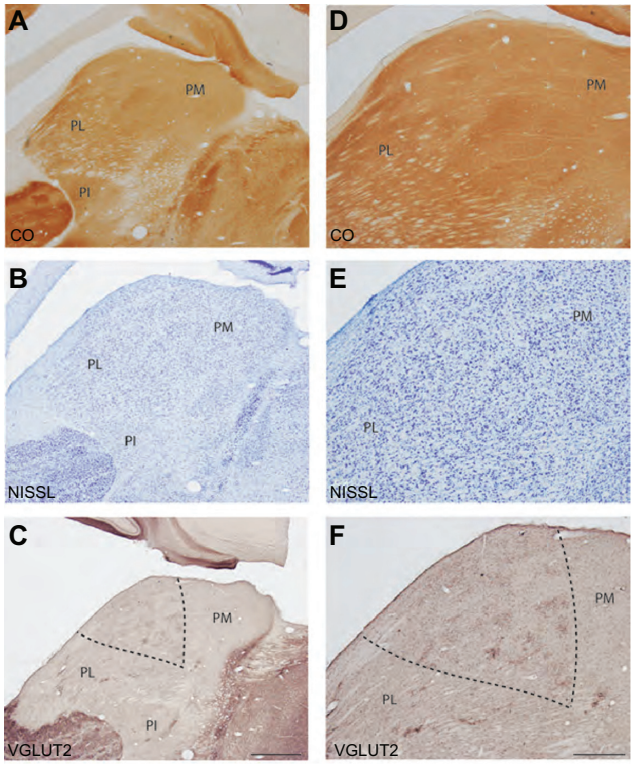

Figure 10 Patchy distribution of VGLUT2 positive terminals in the pulvinar complex. Serial sections of the pulvinar complex in low magnification (**A–C**) and higher magnification (**D–F**) stained for CO (**A, D**), Nissl (**B, E**), and VGLUT2 protein (**C, F**). VGLUT2 staining shows a region between PM and PL with patches of glutamatergic terminals. These could be projections from the ISGS of the SC to the pulvinar. Scale bar is 1 mm (**A–C**) and 0.5 mm (**D–F**).

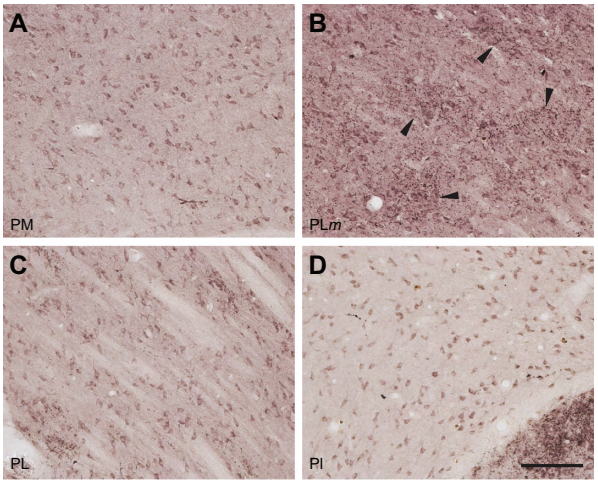

Figure 11 Diffential expression of VGLUT2 protein in each subdivision of the pulvinar complex. **A**) PM shows dense staining of VGLUT2-positive cell bodies. **B**) The medial region of PL shows dense patches of VGLUT2 positive terminals, which could be SC projections to pulvinar. **C**) Lateral PL shows dense VGLUT2 staining of cell bodies and sparse staining of terminals. **D**) Most of PI shows diffuse staining of VGLUT2 cell bodies but lacks VGLUT2 positive terminals. Scale bar is 100 μm.

superior colliculus of prosimian galagos. We find that, similar to rodent studies, both VGLUT2 mRNA and protein are widely expressed in the LGN, SC, and pulvinar. Additionally, the differential distribution of VGLUT2 in the SC and pulvinar allowed us to identify novel subdivisions of each region. Overall, we can conclude that VGLUT2 is the primary glutamate transporter utilized by visual subcortical areas in galagos given its widespread distribution in the afferent and efferent projections of these regions.

Lateral geniculate nucleus

The lateral geniculate nucleus of galagos receives retinal input from both eyes and projects directly to V1. The strong

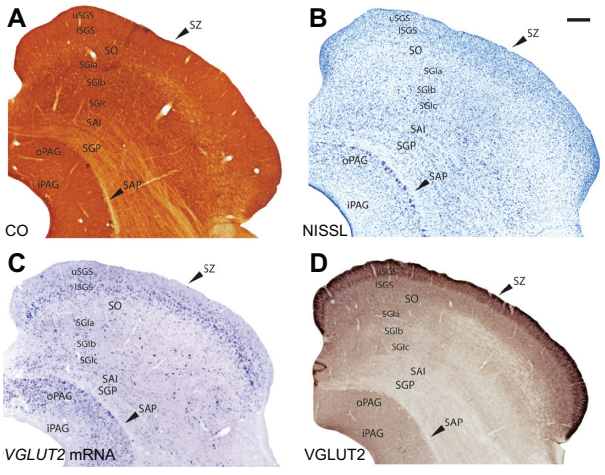

Figure 12 Serial sections through the superior colliculus (SC) stained for (**A**) CO, (**B**) Nisl, (**C**) *VGLUT2* mRNA and (**D**) VGLUT2 protein. Scale bar is 0.5 mm. Coronal sections; medial is right.

expression of *VGLUT2* mRNA and protein in all layers of the LGN indicates that both the retinogeniculate and geniculocortical pathways primarily utilize VGLUT2 to modulate glutamatergic transmission. This is consistent with studies in rodents that showed strong expression of both the protein and the mRNA in both pathways. Although the distribution of VGLUT2 has not been previously characterized in the galago retina, VGLUT2-ir was seen in the ganglion cells of both rat and human retinas,[31] which indicates that retinal projections to the SC and LGN likely utilize VGLUT2 for excitatory transmission. Thus, the strong expression of VGLUT2 protein in the galago LGN likely arises from retinal projections to each layer, which is consistent with the idea that retinogeniculate projections utilize VGLUT2 as their primary glutamate transporter. The LGN of galagos projects to layers IV, VI, III, and I of striate cortex.[32–37] Specifically, M cells project to layer IVα and somewhat to layer IIIC, P cells project to layer IVβ and K cells project to the CO blobs in layer III and layer I. The expression of *VGLUT2* mRNA by M and P cells in the LGN suggests that these geniculostriate projections all use VGLUT2 as their primary glutamate transporter. Previous descriptions of VGLUT2-ir in the neocortex of galagos[7] showed strong, dense labeling of VGLUT2 protein in layer IV of V1. VGLUT2-ir of layer 3 was weak in V1, but moderate staining was present in a patchy pattern possibly corresponding to the blobs where the cells in the K layers project. Overall, we found weak *VGLUT2* mRNA expression in the K layers of the LGN.

Pulvinar

The pulvinar complex of galagos is traditionally organized into three regions, the medial pulvinar, lateral pulvinar and inferior pulvinar,[21,22] although recent studies have been able to further subdivide each of these nuclei in other primates into separate regions based on histochemical and connectional studies.[23] Since we were unable to subdivide the pulvinar past the three traditional regions from our results, we limit our discussion to those divisions. The pulvinar complex of galagos is densely connected with multiple areas of visual and nonvisual cortex.[38] In galagos, the medial pulvinar has reciprocal connections with frontal and parietal cortex, the lateral pulvinar is well connected with early visual areas such as V1, V2, and possibly V3, and the inferior pulvinar is linked to V1 and V2, as well as the middle temporal area (MT) and possibly other higher-order visual areas. The subcortical connections of the pulvinar nucleus of galagos include afferent projections from the lower stratum griseum superficiale of the superior colliculus to the inferior pulvinar.[6] Since VGLUT2 has been

described previously as within subcortical projections to the thalamus and thalamocortical projections in rodents, and not found in corticothalamic projections, it is not surprising that our results show few VGLUT2-positive terminals in the three subdivisions of the pulvinar complex. The localization of VGLUT2-ir to cell bodies and axons instead of terminals is consistent with the evidence that most of the input to the pulvinar is from cortex, and not from subcortical structures such as the superior colliculus. VGLUT2 immunoreactivity in the pulvinar may also arise from intrinsic connections within the nucleus; collateral branches from thalamocortical projections from relay neurons could terminate on nearby inhibitory neurons and have modulatory connections within that subdivision.[25] These intrinsic connections could also be responsible for VGLUT2-ir within this nucleus.

It is surprising that concentrations of VGLUT2-positive terminals did not appear in the inferior pulvinar given its strong connection with the superior colliculus, but these projections might utilize a different form of glutamate transport or a different isoform of the VGLUT family. Additionally, we did find dense patches of VGLUT2-positive terminals in the medial part of the lateral pulvinar, which could be input from the superior colliculus; however, further studies would be required to determine the origin of these dense terminal projections. The strong expression of *VGLUT2* mRNA in all divisions of the pulvinar is consistent with their excitatory projections to cortical areas and corresponds well with the strong VGLUT2 immunoreactivity seen in those cortical areas.[7] Thus, we can conclude that the pulvinar complex utilizes VGLUT2 as its primary glutamate transporter for afferent projections to cortex, but inputs from cortex likely use a different VGLUT isoform in their terminations.

Superior colliculus

The superior colliculus in primates is a complex multisensory structure that receives diverse inputs from cortical and subcortical regions and projects to multiple structures in the central nervous system as well.[26] Visual processing in the superior colliculus is largely restricted to the superficial layers, while the deep layers are responsible for sensorimotor integration and motor functions. In galagos, the primary target of retinal projections in the superior colliculus is the stratum griseum superficiale (superficial gray); the upper sublayer of the superficial gray (uSGS) receives a dense superficial projection of retinal afferents from the contralateral eye, and a deeper projection from the ipsilateral eye, while the lower sublayer (lSGS) receives more diffuse retinal input.[33] As discussed above, retinal ganglion cells likely use VGLUT2 as their primary glutamate transporter, so their terminal distribution in the superior colliculus should also exhibit strong VGLUT2-ir. This is consistent with our findings of dense VGLUT2-ir in the stratum zonale and upper superficial gray and less dense, yet still intense, VGLUT2-ir in the lower superficial gray. The upper and lower superficial gray layers in galagos project to the LGN and the pulvinar respectively.[27,39] Upper superficial gray projections to the LGN primarily terminate on the K layers of the LGN[32] and lower superficial gray projections to the pulvinar mainly target the inferior division.[6] Diffuse staining of *VGLUT2* mRNA in the upper superficial gray corresponds with the sparse VGLUT2-ir seen in the K layers of the LGN, indicating that colliculogeniculate projections do use VGLUT2 for excitatory transmission but at lower levels compared to other projections. The dense staining of *VGLUT2* mRNA in the lower superficial gray, however, seems incongruent with the lack of densely-labeled VGLUT2-positive terminals in the inferior pulvinar described here. The lack of dense staining for VGLUT2-positive terminals in the inferior pulvinar suggests that projections from the lower superficial gray target different regions of the pulvinar complex. As discussed above, the patchy distribution of VGLUT2-positive terminals in the medial part of the lateral pulvinar could reflect the terminations of colliculus projections. The intermediate and deep layers of the superior colliculus are involved in sensory integration and brainstem-related motor functions, which are outside the scope of this discussion, but the laminar distribution of VGLUT2 mRNA and protein is largely consistent with previous findings in rodents.[4] The three subdivisions of the stratum griseum intermediale (intermediate gray) that we see in cytochrome oxidase, *VGLUT2* mRNA and VGLUT2 protein staining is a novel finding in galagos, but has been previously reported in rodents,[40] squirrels,[41] which are rodents with well developed visual systems similar to that of primates, and tree shrews,[42] which are highly visual mammals that are a close relative of the primate lineage. Thus, our identification of three sublamina in the intermediate gray layer is consistent with architectonic divisions of the superior colliculus in closely related species. The division of the periaqueductal gray into inner and outer layers according to *VGLUT2* mRNA expression is also novel in galagos.

Overall, our conclusions on the distribution of *VGLUT2* mRNA and protein expression, and the subsequent visualization of sublamina in the superior colliculus and pulvinar complex of galagos are largely consistent with related studies in rodent and primate species.

Acknowledgments

This work was funded by the National Eye Institute grant EY 02686 to JHK. We thank Laura Trice for assistance in tissue processing and histology and Mary Feurtado for assistance in animal care.

Disclosure

The authors report no conflicts of interest in this work.

References

1. Fremeau RT, Troyer MD, Pahner I, et al. The expression of vesicular glutamate transporters define two classes of excitatory synapse. *Neuron*. 2001;31(2):247–260.
2. Fremeau RT, Voglmaier S, Seal RP, Edwards RH. VGLUTs define subsets of excitatory neurons and suggest novel roles for glutamate. *Trends Neurosci*. 2004;27(2):98–103.
3. Barroso-Chinea P, Castle M, Aymerich MS, et al. Expression of the mRNAs encoding for the vesicular glutamate transporters 1 and 2 in the rat thalamus. *J Comp Neurol*. 2007;501(5):703–715.
4. Kaneko T, Fujiyama F, Hioki H. Immunohistochemical localization of candidates for vesicular glutamate transporters in the rat brain. *J Comp Neurol*. 2002;444(1):39–62.
5. Fremeau RT, Kam K, Qureshi T, et al. Vesicular glutamate transporters 1 and 2 target to functionally distinct synaptic release sites. *Science*. 2004;304(5678):1815–1819.
6. Wong P, Collins CE, Baldwin MKL, et al. Cortical connections of the visual pulvinar complex in prosimian galagos (*Otolemur garnetti*). *J Comp Neurol*. 2009;517(4):493–511.
7. Wong P, Kaas JH. Architectonic subdivisions of neocortex in the galago (Otolemur garnetti). *Anat Rec*. 2010;293(6):1033–1069.
8. Hackett TA, De La Mothe LA. Regional and laminar distribution of the vesicular glutamate transporter, VGLuT2, in the macaque monkey auditory cortex. *J Comp Neurol*. 2009;38(2):106–116.
9. Bai L, Xu H, Collins JF, Ghishan FK. Molecular and functional analysis of a novel vesicular glutamate transporter. *J Biol Chem*. 2001;276(39):36764–36769.
10. Hackett TA, Takahata T, Balaram P. VGLUT1 and VGLUT2 mRNA expression in the primate auditory pathway. *Hear Res*. 2010 Nov 24. [Epub ahead of print].
11. Kaas JH. Evolution of the neocortex. *Curr Biol*. 2006;16(21): R910–R914.
12. Martin RD. Palaeontology: Combing the primate record. *Nature*. 2003;422(6930):388–391.
13. Kaneko T, Fujiyama F. Complementary distribution of vesicular glutamate transporters in the central nervous system. *Neurosci Res*. 2001; 42(4):243–250.
14. Wong-Riley M. Changes in the visual system of monocularly sutured or enucleated cats demonstrable with cytochrome oxidase histochemistry. *Brain Res*. 1979;171(1):11–28.
15. Tochitani S, Liang F, Watakabe A, et al. The occ1 gene is preferentially expressed in the primary visual cortex in an activity-dependent manner: a pattern of gene expression related to the cytoarchitectonic area in the adult macaque neocortex. *Eur J Neurosci*. 2001;13(2): 297–307.
16. Casagrande VA, Kaas JH. The afferent, intrinsic, and efferent connections of primary visual cortex in primates. *Cereb Cortex*. 1994;10:201–259.
17. Kaas JH, Huerta MF, Weber JT, et al. Patterns of retinal terminations and laminar organization of the lateral geniculate nucleus of primates. *J Comp Neurol*. 1978;182(3):517–554.
18. McDonald CT, McGuinness ER, Allman JM. Laminar organization of acetylcholinesterase and cytochrome oxidase in the lateral geniculate nucleus of prosimians. *Neuroscience*. 1993;54(4):1091–1101.
19. Johnson JK, Casagrande VA. Distribution of calcium-binding proteins within the parallel visual pathways of a primate (Galago crassicaudatus). *J Comp Neurol*. 1995;356(2):238–260.
20. Casagrande VA, Joseph P. Morphological effects of monocular deprivation and recovery on the dorsal lateral geniculate nucleus in a galago. *J Comp Neurol*. 1980;194(2):413–426.
21. Norden JJ, Kaas JH. The identification of relay neurons in the dorsal lateral geniculate nucleus of monkeys using horseradish peroxidase. *J Comp Neurol*. 1978;182(4):707–726.
22. Stepniewska I, Kaas JH. Architectonic subdivisions of the inferior pulvinar in New World and Old World monkeys. *Vis Neurosci*. 1997; 14(6):1043–1060.
23. Stepniewska I, Qi HX, Kaas JH. Do superior colliculus projection zones in the inferior pulvinar project to MT in primates? *Eur J Neurosci*. 1999;11(2):469–480.
24. Kaas JH, Lyon DC. Pulvinar contributions to the dorsal and ventral streams of visual processing in primates. *Brain Res Rev*. 2007;55(2): 285–296.
25. Jones E. *The Thalamus*. 2nd ed. New York, NY: Cambridge University Press; 2007.
26. Kaas JH, Huerta MF. Subcortical visual system of primates. In: Steklis, HP, editor. *Comparative Primate Biology*. *Vol.4: Neurosciences*. New York, NY: Alan R Liss, Inc; 1988.
27. May PJ. The mammalian superior colliculus: laminar structure and connections. *Prog Brain Res*. 2006;151:321–378.
28. Raczkowski D, Diamond IT. Cells of origin of several efferent pathways from the superior colliculus in Galago senegalensis. *Brain Res*. 1978;146(2):351–357.
29. Ortega F, Hennequet L, Sarria R, et al. Changes in the pattern of glutamate-like immunoreactivity in rat superior colliculus following retinal and visual cortical lesions. *Neuroscience*. 1995;67(1):125–134.
30. Schönitzer K, Höllander H. Retinotectal terminals in the superior colliculus of the rabbit: a light and electron microscopic analysis. *J Comp Neurol*. 1984;223(2):153–162.
31. Gong J, Jellali A, Mutterer J, et al. Distribution of vesicular glutamate transporters in rat and human retina. Brain Res. 2006;1082(1):73–85.
32. Glendenning KK, Kofron EA, Diamond IT. Laminar organization of projections of the lateral geniculate nucleus to the striate cortex in Galago. *Brain Res*. 1976;105(3):538–546.
33. Casagrande VA, DeBruyn EJ. The galago visual system: aspects of normal organization and developmental plasticity. In: Haines DE, editor. *The Lesser Bushbaby (Galago) as an Animal Model: Selected topics*. Boca Raton, FL: CRC Press; 1982:137–168.
34. Florence SL, Sesma MA, Casagrande VA. Morphology of geniculostriate afferents in a prosimian primate. *Brain Res*. 1983;270(1): 127–130.
35. Florence SL, Casagrande VA. Organization of individual afferent axons in layer IV of striate cortex in a primate. *J Neurosci*. 1987;7(12): 3850–3868.
36. Diamond IT, Conley M, Itoh K, et al. Laminar organization of geniculocortical projections in Galago senegalensis and Aotus trivirgatus. *J Comp Neurol*. 1985;242(4):584–610.
37. Lachica EA, Casagrande VA. Direct W-like geniculate projections to the cytochrome oxidase (CO) blobs in primate visual cortex: axon morphology. *J Comp Neurol*. 1992;319(1):141–158.
38. Stepniewska I. The pulvinar complex. In: Kaas JH, Collins CE, editors. *The Primate Visual System*. Boca Raton, FL; CRC Press; 2004.
39. Harting JK, Huerta MF, Hashikawa T, et al. Projection of the mammalian superior colliculus upon the dorsal lateral geniculate nucleus: organization of the tectogeniculate pathways in nineteen species. *J Comp Neurol*. 1991;304(2):275–306.

40. Helms MC, Ozen F, Hall WC. Organization of the intermediate gray layer of the superior colliculus. I. Intrinsic vertical connections. *J Neurophysiol*. 2004;91(4):1706–1715.
41. Baldwin MK, Wong P, Reed JL, Kaas JH. Superior colliculus connections with visual thalamus in gray squirrels (Sciurus carolinensis): Evidence for four subdivisions within the pulvinar complex. *J Comp Neurol*. 2011;519(6):1071–94.
42. Harting JK, Diamond IT, Hall WC. Anterograde degeneration study of the cortical projections of the lateral geniculate and pulvinar nuclei in the tree shrew (Tupaia glis). *J Comp Neurol*. 1973;150(4):393–440.